A TSO-DSO Coordination Platform with Reserve Deliverability and AC Distribution Systems

Zejun Ruan, Anthony Papavasiliou, *Senior Member*, Dimitris Krithis

***Abstract*—This paper proposes a scalable, economically disciplined framework for implementing flexibility platforms that coordinate distributed energy resources across transmission and distribution networks. Our proposed platform models reserve deliverability, relies on decentralized PTDF and pricing computations, checks for AC feasibility, and is demonstrated on a realistic country-scale TSO-DSO coordination case study. The proposed market-clearing formulation co-optimizes energy and reserves under network constraints and confirms incentive alignment via a lost opportunity cost metric. We implement a Benders decomposition algorithm in order to achieve computational scalability and validate our approach using a detailed test system of TSO-DSO coordination in Belgium. Comparative analysis with alternative platform designs highlights the superior trade-off of our framework between operational efficiency and network security.**

***Index Terms*—Reserve deliverability, TSO-DSO coordination, balancing markets, flexibility markets, congestion management, scarcity pricing, co-optimization of energy and reserve, AC power flow.**

I. Introduction

A. Motivation

Flexibility platforms for mobilizing distribution system flexibility have grown rapidly in recent years. This expansion is driven by the increasing integration of both generation resources (e.g. rooftop solar) as well as flexibility resources (e.g. electric vehicles) at medium and low-voltage grid levels. This rapid integration of distributed energy resources (DERs) is inducing stress on transmission and distribution networks at a pace that network operators struggle to keep up with. The expansion of existing distribution network infrastructure is not deemed as a sustainable solution in this context, both due to construction delays that fail to keep up with the pace of distributed resource integration, but also due to excessive capital investment in idle network capacity [1]. In a likely future where the increased amount of DERs at the distribution level supplies a non-negligible share of energy to the power system, it is necessary to consider (i) the influence of distribution-level DERs on wholesale energy and flexibility markets, (ii) the impact of these DERs on the distribution network and (iii) the interaction between transmission and distribution system operators (TSO and DSO). This paper proposes a secure and incentive-compatible TSO-DSO coordination framework designed for computational scalability in large-scale power systems as a practical implementation of the theoretical advancements in reserve deliverability [2], [3].

The continuously growing importance of the discussed subject is highlighted by the amount of completed or ongoing flexibility platform projects, detailed in various reviews [4]–[6]. The European flexibility platforms that are presented in these surveys share two fundamental commonalities: an inherent locational dependency and a requirement for timely operational delivery. The geographical nature of these platforms and their performance-based remuneration are considered crucial among practitioners, not only for guaranteeing the reliable short-term provision of resources, but also for structuring effective signals for optimal investments in flexible resources across precise locations within the network.

Distribution locational marginal pricing (DLMP) [7]–[13] can deliver on the desiderata of the aforementioned locational differentiation and paying for performance. This can be achieved by (i) solving an integrated optimal power flow that accounts for both transmission as well as distribution networks (thereby enabling the formation of distribution locational marginal prices), (ii) introducing an operating reserve demand curve (ORDC) [14] at the high-voltage transmission system (which allows for locational marginal prices to be uplifted by the price of reserve under conditions of reserve scarcity), and (iii) introducing endogenous reserve deliverability constraints within the market clearing model [7]. This enables reserve scarcity adders to propagate *only* to parts of the network where flexibility resources can actually deliver useful services to the grid, as opposed to also paying flexible resources that are located behind systematically congested distribution lines.

The disciplined implementation of such a TSO-DSO coordination framework requires solving the aforementioned market clearing model in real time. There are various institutional deviations from existing European market arrangements. (i) European markets do not implement locational marginal pricing (although the aforementioned flexibility platforms are either implicitly or explicitly allowing for the emergence of locational prices at distribution level). (ii) European markets do not co-optimize energy and reserve in the day ahead or in real time. The integrated day-ahead European market focuses on energy alone, without accurately representing physical network constraints. And the real-time market does not trade reserve in Europe.

Bridging these deviations requires two key transitions: the shift from zonal to nodal market clearing, and co-optimization of energy and reserves. To safely increase spatial granularity without jeopardizing market liquidity, three structural reforms are prerequisite [15]: shifting from physical to financial balancing groups, replacing block-based complex bids with unit-based multi-part bids, and utilizing intraday auctions closer to real time for efficient capacity allocation. Regarding co-optimization, advanced bidding structures that allow generators and flexible resources to offer capacity across both energy and reserve markets are required, alongside dynamic transmission capacity allocation (e.g., to automatically determine whether interconnections are best used for flowing energy or sharing reserves) [16]. Robust pricing rules to manage inherent market non-convexities, such as minimum generation levels and start-up costs, are also necessary.

Despite these institutional deviations between EU market design and the proposal set forth in this work, we nevertheless consider it a complete and disciplined framework for implementing distribution-level flexibility markets that appropriately account for network and generation scarcity. Our method addresses the network-aware pricing needs of emerging European flexibility platforms. It is worth noting that a precursor of the approach that we develop in this paper has been examined in the context of transmission-distribution coordination through our collaboration with Statnett and Tensio in Norway [17].

B. Related Literature

TSO-DSO coordination mechanisms have been studied extensively in the literature [7], [18]–[22]. Gerard et al. [18] introduce several possible coordination schemes. Among related works, Yuan et al. [19] propose a scalable hierarchical scheme using SOCP-based ACOPF that co-optimizes energy and reserve capacity but does not address reserve deliverability. Bragin et al. [23] dynamically linearize the AC representation and decompose via Lagrangian Relaxation, prioritizing AC feasibility but omitting reserves and limiting scalability. Mohammadi et al. [20] and Mezghani et al. [21] propose decentralized TSO-DSO frameworks, the former using Analytical Target Cascading and the latter having DSOs submit grid-secure residual supply functions, but neither includes reserve provision. Jiang et al. [22] co-optimize energy and reserves at the TSO level with an SOCP-relaxed DSO, formulating the problem as a single-level MISOCP that ensures deliverability but does not scale to large networks.

Our proposed model is inspired by the framework of [7], who envision a distributed market clearing framework that jointly optimizes energy and reserves for both transmission and distribution systems while accounting for reserve deliverability[1].

Regarding DLMP computation specifically, several alternative approaches exist. Wang et al. [25] depart from the stochastic formulation of [7] by proposing a robust optimization model that treats both energy and reserves. Other works focus on the energy side alone: Li et al. [9] address active power and congestion management, while Huang et al. [11] extend the formulation to capture voltage and reactive power through an MISOCP model, resolving the issue of multiple optimal dispatch schedules. Yuan et al. [12] and Bai et al. [13] similarly rely on SOCP formulations with hierarchical decomposition. A common limitation across these works is that none simultaneously addresses reserve deliverability at the distribution level.

[1]Reserve deliverability refers to the practice of committing reserves in a way that accounts for the ability of the network to deliver committed reserves at different parts of the system [7], [24].

Reserve deliverability itself is widely studied [7], [24], [26]–[28], yet a methodological gap remains in achieving computationally tractable formulations at the distribution level. Most existing models co-optimize energy and reserves at the transmission level using computationally intensive scenario-based, zonal, or robust approaches [24], [26], [27]. Our work in [3] demonstrates that reserve deliverability can be effectively approximated without resorting to such formulations; in the current paper we propose using this approach for distribution system flexibility. At the distribution level, Caramanis et al. [7] ensure deliverability through a discrete set of scenarios with distribution voltage constraints and line limits enforced, while Paredes et al. [28] follow a sequential clearing structure where energy activation depends on previously cleared capacity.

C. Contributions

(i) *Modeling*. Building upon the inscribed boxes (IB) model originally described in [3], we formulate a novel market-clearing approach for TSO-DSO coordination which accounts for numerous detailed aspects of system operation (day-ahead followed by real-time operation, AC power flow, upward and downward reserve activations). (ii) *Computational*. We develop a decomposition algorithm which is compatible with information sharing constraints of TSOs and DSOs and deploy the proposed algorithm on parallel computing infrastructure. We provide a proof of concept by applying this algorithm to a realistic case study of a national power grid with 360 distribution networks. (iii) *Policy*. We benchmark our proposal against two TSO-DSO interaction alternatives considered through collaboration with industry. The effectiveness of the proposed design is established through a comprehensive evaluation of four key performance metrics: system security, economic efficiency, incentive compatibility (measured via lost opportunity costs), and computational scalability. A novel insight of this benchmarking is that, although the alternative proposals can perform well along certain metrics under specific network conditions, the proposed design is robust with respect to all metrics under all system conditions.

II. MODELS

In this section, we formulate our proposed model for the coordinated clearing of transmission and distribution while accounting for reserve deliverability. The proposed framework in Sections II-B to II-D is illustrated in Fig. 1.

A. Notation summary

A brief summary of notation is provided in this section.

- N, N_{DN}, N_{TN}: 1) Set of buses in both the transmission and distribution networks; 2) Set of buses in distribution networks; 3) Set of buses in the transmission network.
- *US*: Set of generators
- K, K_{DN}, K_{TN}: 1) Set of lines in both the transmission and distribution network; 2) Set of lines in the distribution network; 3) Set of lines in the transmission network
- RL: Set of segments in operating reserve demand curve.
- B_g, FB_k, TB_k: 1) The bus that asset g is located at; 2) FB_k is from bus and 3) TB_k the to bus for a line $k \in K$.

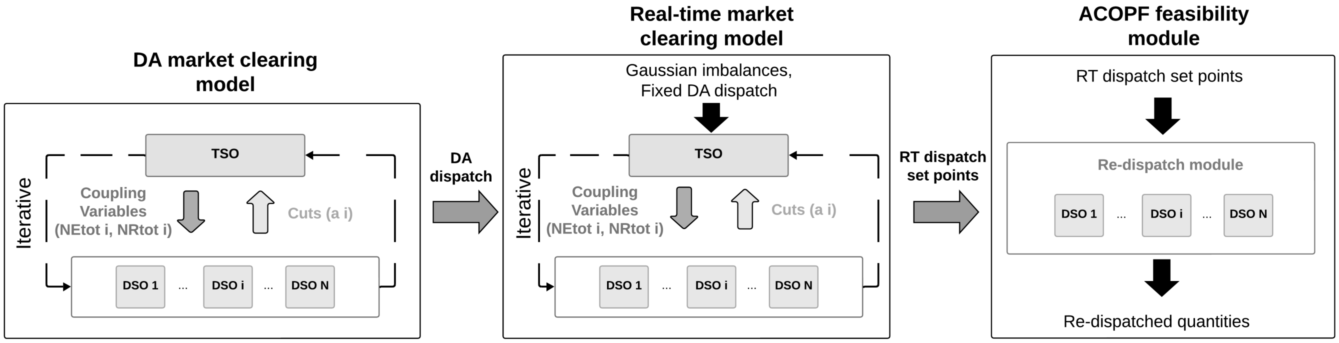

Fig. 1. Schematic diagram of the interaction between the components of the proposed framework.

- PR_i: Reserve valuation of ORDC segment i.
- MC_g: Marginal cost of generator g.
- QR_i, P_g^+, P_g^-, , P_g^0: 1) Reserve quantity offered for a certain ORDC segment; 2) Maximum active power quantity a generator at bus n is able to offer; 3) Minimum active power quantity of a generator at bus n; 4) Active power position of generator g.
- F_k^+: Maximum capacity of line k.
- P_n, D_n: Day-ahead power production/consumption at bus n.
- $NEtot_i, NRtot_i$: 1) Total energy net injection import from a distribution network i to the transmission network; 2) Total reserve net injection import from a distribution network i to the transmission network
- S_{nm}, I_{nm}, Z_{nm}: 1) Apparent flow on a line from node n to m; 2) Current flow on a line from node n to m; 3) Impedance of line from node n to m.
- $p_g^{redisp}, q_g, v_n, \theta_n$: 1) Real power re-dispatched of generator g; 2) Reactive power produced of generator g; 3) Voltage magnitude at bus n; 4) Voltage angle at bus n
- p_g: Real power production variable of generator g
- r_g, dr_l: 1) Upward reserve quantity offered from generator g; 2) The quantity of upward reserve demand of order $l \in RL$ that is served.
- ne_n, nr_n: 1) Energy injection at bus n; 2) Upward reserve injection at bus n.
- fr_k^+, fr_k^-: 1) Reserve flow on the reference direction of line k; 2) Reserve flow on the opposite of the reference direction of line k.

B. Day-ahead market clearing model

In this section we proceed to present a TSO-DSO coordination model that co-optimizes energy and reserve, while considering reserve deliverability. While maintaining the core concept of stochastic formulations [7], our method adopts a distinct perspective, leveraging the concept of inscribed boxes. The idea is detailed in [3].

The model is formulated as follows:

$$\max_{p,r,dr,ne,nr,fr^{+/-}} \sum_{l\in RL} PR_l \cdot dr_l - \sum_{g\in US} MC_g \cdot p_g \quad (1)$$

$$(\lambda_n): ne_n = \sum_{g\in US:B_g=n} p_g + P_n - D_n, \quad n\in N \quad (2)$$

$$(\lambda R_n): nr_n = \sum_{g\in US:B_g=n} r_g - \sum_{l\in RL:B_l=n} dr_l, \quad n\in N \quad (3)$$

$$(\sigma): \sum_{n\in N} ne_n = 0 \quad (4)$$

$$(\kappa_n): \; nr_n = \sum_{k\in K:FB_k=n} fr_k^+ - \sum_{k\in K:TB_k=n} fr_k^+ + \sum_{k\in K:FB_k=n} -fr_k^- - \sum_{k\in K:TB_k=n} -fr_k^-, \quad n\in N_{DN} \quad (5)$$

$$(\phi_k^+): \; \sum_{n\in N} PTDF_{n,k}\cdot ne_n + \sum_{k'\in K} \max(A_{k,k'},0)\cdot fr_{k'}^+ + \sum_{k'\in K} \max(-A_{k,k'},0)\cdot fr_{k'}^- \le F_k^+, \quad k\in K_{DN} \quad (6)$$

$$(\phi_k^-): \; \sum_{n\in N} -PTDF_{n,k}\cdot ne_n + \sum_{k'\in K} \max(A_{k,k'},0) \cdot fr_{k'}^- + \sum_{k'\in K} \max(-A_{k,k'},0)\cdot fr_{k'}^+ \le F_k^-, \quad k\in K_{DN} \quad (7)$$

$$(\xi_k^+): \; \sum_{n\in N} PTDF_{n,k}\cdot ne_n \le F_k^+, \quad k\in K_{TN} \quad (8)$$

$$(\xi_k^-): \; \sum_{n\in N} -PTDF_{n,k}\cdot ne_n \le F_k^-, \quad k\in K_{TN} \quad (9)$$

$$(\mu_g^+): p_g + r_g \le P_g^+, \quad g\in US \quad (10)$$

$$(\mu_g^-): p_g \ge P_g^-, \quad g\in US \quad (11)$$

$$(\psi_l): dr_l \le QR_l, \quad l\in RL \quad (12)$$

$$r,\; dr,\; fr^+,\; fr^- \ge 0 \quad (13)$$

The proposed model identifies the maximum volume box within the feasible space of bilateral reserve exchanges. These feasible injections are constrained by DC power flow constraints. The exchanges are determined by the flow variables fr_k. Thus, we can replace the nr_n variables by the fr_k variables in the power flow constraints, based on Eq. (5).

This substitution leads to the definition of parameters $A_{k,k'} = PTDF_{FB_{k'},k} - PTDF_{TB_{k'},k}$, $\forall k, k' \in K$. Intuitively, these parameters preserve the effect of a power injection on a network element when the effect is adverse (i.e. when power flows in the direction of the constraint that we are trying to respect) but does not preserve the effect when it is beneficial (i.e. counter-flows on a line are ignored/eliminated). The objective function of the model in Eq. (1) maximizes welfare. The first term corresponds to the benefit acquired by the system operator for fulfilling the demand of an operating reserve demand curve for upward reserve while the second term corresponds to the fuel cost of generators. Note that the conceptualization of the ORDC is based on internalizing real-time uncertainty in a computationally scalable and institutionally acceptable market clearing model. This is detailed in Hogan's derivation of the ORDC from a two-stage stochastic economic dispatch model [14]. Eqs. (6), (7) guarantee that reserves are matched such that the potential activation of reserves results in line loadings that respect line constraints. Eqs. (2),(3) are energy and reserve balance constraints, respectively. Eqs. (8) and (9) correspond to line capacity constraints at the transmission level for each line k. Eqs. (10), (11) correspond to generator capacity constraints. The remaining Eq. (12) represents the maximum reserve demand of the l-th segment of the ORDC.

C. Intuition of the Inscribed-Boxes formulation

To illustrate the inscribed boxes formulation, we provide a 3-node example inspired by [29]. The system, depicted in Fig. 2, features a reserve demand at node 3 capable of consuming up to 550MW, while generators G1 and G2 can provide up to 500MW and 200MW, respectively. We assume identical line characteristics and consider the flow limits for lines 1-2, 2-1, 2-3, 3-1.

For the stochastic formulation described in [3], the flow-based polytope is defined by $\sum_{n \in N} PTDF_{n,k} \cdot ne_{n,s} \leq F_k^-, k \in K$ $(*)$, where s is the scenario index. The activation scenario set consist of two scenarios, scenario 1 where DR3 activates and scenario 0 where it does not. For scenario 0, it is trivial to observe that $(*)$ is satisfied, as no node exports or imports energy. We drop the scenario index for ease of exposition and for scenario 1 $(*)$ becomes:

$$0.33 \cdot ne_1 - 0.33 \cdot ne_2 \leq 100 \tag{14}$$
$$0.33 \cdot ne_1 + 0.66 \cdot ne_2 \leq 220 \tag{15}$$
$$-0.33 \cdot ne_1 + 0.33 \cdot ne_2 \leq 100 \tag{16}$$
$$0.66 \cdot ne_1 + 0.33 \cdot ne_2 \leq 300 \tag{17}$$

Given these constraints, the optimal allocation is for G1 to produce 380MW and for G2 to produce 140MW, since the export from node 2 alleviates stress on line 1-2 in equation (14). For scenario 0, the system is also feasible as it can simply reduce all allocated exports to 0.

By comparison, the inscribed-boxes model represents the union of all boxes $\mathcal{B}(l, u) = \{x \in \mathbb{R}^2 : l \leq x \leq u\}$ contained in the polytope of feasible flows with $l = (0, 0)$. This set is defined by:

$$0.66 \cdot fr_{1-2} + 0.33 \cdot fr_{1-3} \leq 100 \tag{18}$$

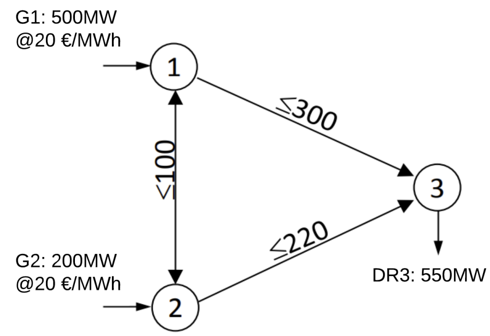

Fig. 2. Three-node example illustrating the concept of inscribed boxes.

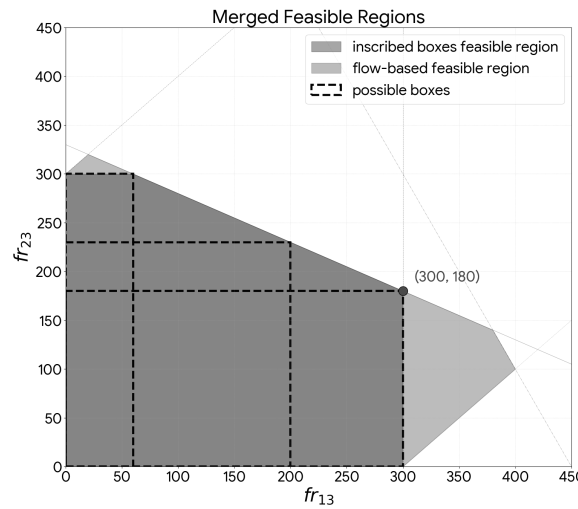

Fig. 3. Feasible region of flows for the example of Fig. 2 for the different scenarios of demand activation (light green) and its inscribed boxes approximation (dark green).

$$0.66 \cdot fr_{2-1} + 0.33 \cdot fr_{2-3} \leq 100 \tag{19}$$
$$0.66 \cdot fr_{2-3} + 0.33 \cdot fr_{2-1} + 0.33 \cdot fr_{1-3} \leq 220 \tag{20}$$
$$0.66 \cdot fr_{1-3} + 0.33 \cdot fr_{1-2} + 0.33 \cdot fr_{2-3} \leq 300 \tag{21}$$

As shown in Fig. 3, this formulation yields an optimal production of 300MW from G1 and 180MW from G2. Any additional allocation from G1 would violate constraint (20). While the solution (300, 180) falls within the feasible region of the original polytope (light green), the inscribed-boxes approach provides a more conservative boundary. Notably, as demonstrated in [2], this approximation is exact for radial networks, making it an attrative formulation for incorporating reserve deliverability in radial distribution networks.

D. Lost opportunity cost

We introduce lost opportunity cost (LOC) as a metric of the quality of our derived prices. LOC quantifies the extent to which the primal solution (decision variables) and the dual solution (prices) are aligned with the surplus maximization incentives of agents given the market dispatch. This metric specifically quantifies the financial loss of a market participant that follows the platform orders instead of its own profit-maximizing actions. We distinguish three types of LOC: one for generators (Generator LOC), one for the network (Network LOC), introduced by [30], and one for the transmission system operator that procures reserve (Reserve buyer LOC). In the following subsections, we present in detail the exact optimization problem that is solved for calculating LOC in all three cases. We denote the dispatch solutions for the market platform with a hat, $\hat{x}$, and the solutions of the selfish surplus maximization problems defined below with a tilde, $\tilde{x}$.

1) Generator LOC: When facing an energy price λ and a reserve price λR, the goal of a generator is to maximize profit. Assuming that the dispatch solutions have been computed, the *potential* profit of a generator $g \in US$ can be computed by solving the following optimization problem:

$$\max_{p,r} Profit_g(p_g, r_g; \lambda, \lambda R) = \\ = \max_{p,r} (\lambda_{B_g} - MC_g) \cdot p_g + \lambda R_{B_g} \cdot r_g \quad (22)$$

$$\text{s.t.} \quad \text{Eqs. } (10), (11) \quad (23)$$

The solution of the aforementioned model is the selfish profit-maximizing action of the generator. It yields a profit of $Profit_g(\tilde{p_g}, \tilde{r_g}; \lambda, \lambda R)$, and has to be compared to the profit achieved when following the dispatch instructions of the market operator, $Profit_g(\hat{p_g}, \hat{r_g}; \lambda, \lambda R)$. The LOC of generator g is then defined as follows:

$$LOC_g(\lambda, \lambda R) = \\ Profit_g(\tilde{p_g}, \tilde{r_g}; \lambda, \lambda R) - Profit_g(\hat{p_g}, \hat{r_g}; \lambda, \lambda R)$$

2) Network LOC: In the same spirit as for generators, we consider the LOC of the network operator as the *potential* arbitrage profit that can be achieved by trading energy and reserve in different parts of the network:

$$\max_{ne,nr} Profit_{NO}(ne, nr; \lambda, \lambda R) = \\ = \max_{ne,nr} - \sum_{n \in N} \lambda_n \cdot ne_n - \sum_{n \in N} \lambda R_n \cdot nr_n \quad (24)$$

$$\text{s.t.} \quad \text{Eqs. } (2) - (9), (13) \quad (25)$$

The solution of the model is denoted as $Profit_{NO}(\tilde{ne}, \tilde{nr}; \lambda, \lambda R)$. The LOC for the network operator is defined as follows:

$$LOC_{NO}(\lambda, \lambda R) = \\ Profit_{NO}(\tilde{ne}, \tilde{nr}; \lambda, \lambda R) - Profit_{NO}(\hat{ne}, \hat{nr}; \lambda, \lambda R)$$

3) Reserve buyer LOC: When facing a reserve price λR, the goal of the agent which procures reserve is to maximize the benefit of securing reserve. The potential surplus of the agent can be computed by the following optimization problem:

$$\max_{dr \geq 0} Profit_{rq}(dr; \lambda R) = \max_{dr \geq 0} \sum_{i \in RL_n} (PR_i - \lambda R_n) \cdot dr_i$$

$$\text{s.t.} \quad \text{Eq. } (12) \quad (26)$$

The solution of the model is denoted as $Profit_{rq}(\tilde{dr}; \lambda R)$. The LOC for the reserve agent is defined as follows:

$$LOC_{rq}(\lambda R) = \\ Profit_{rq}(\tilde{dr}; \lambda R) - Profit_{rq}(\hat{dr}; \lambda R)$$

Given a market clearing solution $\hat{x}$, the total LOC is computed as the following sum:

$$LOC(\lambda, \lambda R) = \\ LOC_{NO}(\lambda, \lambda R) + \sum_{g \in US} LOC_g(\lambda, \lambda R) + LOC_{rq}(\lambda R)$$

E. Real-time modules

In real time we run two modules. One is a real-time market clearing module, which is used for determining the setpoint of different units in real time against real-time system conditions. Given these setpoints, we then run an AC power flow, in order to quantify the amount of redispatch which is required in order to restore feasibility.

Real-time market clearing. For the real-time market module, we draw Gaussian imbalances that are generated using the same underlying probability density function as the one used for calibrating the ORDC. The real-time module also considers free bids (i.e. participation of resources that have not been committed for reserves but are flexible) and accounts for line capacity constraints. In essence, the real-time power flow model that we solve mirrors the one described in section II-B. However, it is solved by fixing the day-ahead energy position of the generators, dropping the dr variables and introducing imbalances.

AC power flow feasibility. To assess real-time operational security, an AC power flow re-dispatch module is incorporated to quantify network violation at the distribution level. This module, presented analytically in section V of [31], is based on the classical formulation of AC-PF and decides on variables p^{redisp}, q, v, θ. The dispatch decisions of a generator g from the day-ahead and real-time markets are incorporated through parameter P_g^0.

III. Decentralization

An important advantage of our day-ahead market clearing model is that it is decentralized. This allows for scaling the model up to networks of arbitrary size, and limiting information sharing between transmission and distribution system operators.

A. Decomposition of day-ahead market clearing model

In this section, a Benders [32] decomposition is applied to the proposed day-ahead market clearing model. The Benders master problem in our case is the transmission system problem and the slave problems are the distribution system problems. The coupling variables are ne_i^{tot}, nr_i^{tot} for $i \in DNs$. The variable a is an auxiliary variable representing the value function of the follower problem in the master-level formulation. The coupling first-stage decision variables that are fixed in the follower problems are defined as $NEtot_i$, $NRtot_i$ for $i \in DNs$. The decomposed model is formulated as follows:

Master:

$$\min_{dr,p,r,a} \sum_{g \in US_{TN}} MC_g \cdot p_g - \sum_{i \in ORDC} PR_i \cdot dr_i + \sum_{i \in DNs} a_i \quad (27)$$

$$s.t. \quad (2),(3),(10)-(12) \tag{28}$$

$$(\xi_k^+): \sum_{n \in N_{TN}} PTDF_{n,k} \cdot ne_n + \sum_{i \in DNs} PTDF_{i,k} \cdot ne_i^{tot} \leq F_k^+, \quad k \in K_{TN} \tag{29}$$

$$(\xi_k^-): \sum_{n \in N_{TN}} -PTDF_{n,k} \cdot ne_n - \sum_{i \in DNs} PTDF_{i,k} \cdot ne_i^{tot} \leq F_k^-, \quad k \in K_{TN} \tag{30}$$

$$\sum_{n \in N_{TN}} ne_n = -\sum_{i \in DNs} ne_i^{tot} \tag{31}$$

$$\sum_{n \in N_{TN}} nr_n = -\sum_{i \in DNs} nr_i^{tot} \tag{32}$$

$$a_i \geq \sum_{g \in US_i} MC_g \cdot p_g + \pi e_i (ne_i^{tot} - \mathit{NEtot}_i) + \pi r_i (nr_i^{tot} - \mathit{NRtot}_i), \quad i \in DNs \tag{33}$$

$$dr, r, a \geq 0 \tag{34}$$

For each distribution network i, the subproblem is formulated as follows:

Slave:

$$V_i(\mathit{NEtot}_i, \mathit{NRtot}_i) = \min_{p,r \geq 0} \sum_{g \in US_i} MC_g \cdot p_g \tag{35}$$

$$s.t. \quad (2),(3),(10),11), (5)-(7) \tag{36}$$

$$(\pi e_i): \sum_{n \in N_i} ne_n = \mathit{NEtot}_i \tag{37}$$

$$(\pi r_i): \sum_{n \in N_i} nr_n = \mathit{NRtot}_i \tag{38}$$

A minor adjustment is necessary for the master problem in Eqs. (29), (30) compared to Eqs. (8), (9). This adjustment arises from the fact that Eqs. (8), (9) incorporate the sum of *all* N nodes in the meshed network, whereas the master problem only considers transmission nodes. This issue is addressed by the simple addition of the second left-hand-side term of Eqs. (29), 29, by utilizing the fact that (i) we can replace the sum of all nodes of a distribution network i with the coupling variable $ne_i^{tot} = \sum_{n \in D_i} ne_n$ for $i \in$ DNs and (ii) as analyzed in section III-B, the PTDF value of a transmission line k with respect to a distribution node n is exactly the same as the PTDF value of line k with respect to the transmission node that is connected to the distribution network that node n belongs to. An appealing aspect of this approach is that it can be closely interpreted as the submission of aggregated distribution level bids to a wholesale market where transmission assets already operate, which implies that the decomposition proposed above can be approximately implemented with existing European wholesale market operations if the residual supply functions of the slave problems are used as bids in the wholesale market. We explain this point in further detail in [17].

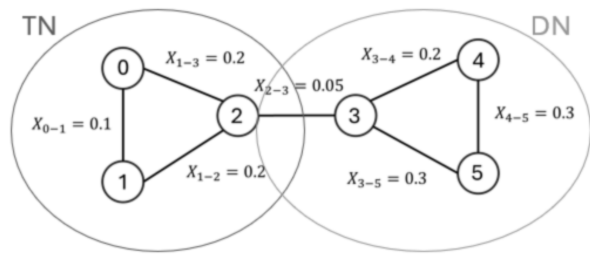

Fig. 4. An illustrative transmission network connected radially to a distribution network which is discussed in Section III-B.

B. Decentralized PTDF computation

This section describes a decentralized method for the calculation of the monolithic PTDF matrix. Given that the transmission network is connected with distribution systems via individual network elements (transformers), the proposed approach formalizes the partitioning of the PTDF matrix into separate computations for each system. This allows for the scalable decomposed model proposed in section III-A to be implemented without transmission and distribution system operators having to share information about their subnetworks. Although the result is highly intuitive, the authors are not aware of a formal statement and proof in the literature.

Proposition 1. *In a meshed network where the transmission system is connected radially to distribution systems (via single interconnections), the monolithic PTDF matrix can be calculated in a decentralized manner by computing the individual PTDF matrices for each system.*

Proof. The analytical proof is provided in the Appendix [31]. □

In order to clarify the main idea of the result, we proceed to present the PTDF matrix structure for a small case of a single transmission and distribution network, as depicted in Fig. 4.

The PTDF matrix obeys the following structure:

$$\begin{bmatrix} PTDF_{TN} & C_{PTDF} \\ 0 & PTDF_{DN}^{aug} \end{bmatrix}$$

Here, $PTDF_{DN}^{aug}$ is the $PTDF$ matrix of the DN, when the distribution interconnecting node is the hub node, augmented by adding one extra row (1X3) of **-1** elements and one extra column of **0** (3X1). $PTDF_{TN}$ is the $PTDF$ matrix of the TN and C_{PTDF} is a (3×3) matrix, where each line has repeated elements.

The full $PTDF$ matrix of the example, which includes node 0 as a hub node, has the following form:

$$\begin{array}{c} \\ \text{Line 0-1} \\ \text{Line 0-2} \\ \text{Line 1-2} \\ \text{Line 2-3} \\ \text{Line 3-4} \\ \text{Line 4-5} \\ \text{Line 3-5} \end{array} \begin{array}{c} \begin{array}{ccccc} \text{Bus 1} & \text{Bus 2} & \text{Bus 3} & \text{Bus 4} & \text{Bus 5} \end{array} \\ \begin{bmatrix} -0.8 & -0.4 & -0.4 & -0.4 & -0.4 \\ -0.2 & -0.6 & -0.6 & -0.6 & -0.6 \\ 0.2 & -0.4 & -0.4 & -0.4 & -0.4 \\ 0 & 0 & -1 & -1 & -1 \\ 0 & 0 & 0 & -0.75 & -0.375 \\ 0 & 0 & 0 & 0.25 & -0.375 \\ 0 & 0 & 0 & -0.25 & -0.625 \end{bmatrix} \end{array}$$

The matrix is structured such that rows 1 through 3 correspond to lines at the transmission level, rows 5 through 7 represent lines at the distribution level, and row 4 is the interconnection. Similarly, columns 1 through 2 correspond to transmission-level buses, and columns 4 through 5 correspond to distribution-level buses.

Each line of matrix C_{PTDF} (3X3) consists of the PTDF value of the interconnecting transmission node 2 to which the DN is connected to. This is because 1 MW of injection at the distribution level influences the transmission line identically to an injection originating from node 2. As mentioned above, the matrix $PTDF_{DN}^{aug}$ matrix consists of the matrix $PTDF_{DN}$ (3X2) in addition to one extra row and column. The intuition behind the value -1 that 1 MW of injection at a distribution node requires that all the injected power flows through the interconnection to reach the hub node. Conversely, the PTDF value of node 3 is zero across all distribution lines, since 1 MW of injection there does not cause any flow through any distribution lines. As expected, $PTDF_{TN}$ (3X2) is the $PTDF$ matrix of the TN with node 0 as the hub node.

Based on the preceding discussion, we conclude that the monolithic PTDF matrix can be constructed only by knowing the PTDF matrices of each network and allows for the Benders decomposition of the previous section where the total net injection variables ne^{tot} and nr^{tot} are used in constraints (29)-(33).

C. Decentralized price computation

In this section, a decentralized price computation approach is proposed. The general idea is that, after solving the primal dispatch model proposed in subsection III-A, all primal and dual variables of the master problem can be retrieved. These can then be used to solve a linear system of the KKT equations that are associated with the distribution systems, thereby obtaining the DLMPs $(\lambda, \lambda R)$. We denote with *hat* the primal and dual variables that are fixed. The decentralized pricing model is presented below.

Given the assumption that each distribution network connects to a unique transmission node via a single link, and that the root node of each distribution network i is a transmission node, the KKT conditions of the slave problem include the following:

$$-\hat{\lambda}_i + \pi e_i = 0 \tag{39}$$

$$-\lambda\hat{R}_i + \pi r_i = 0 \tag{40}$$

Here, $\hat{\lambda}_i$ and $\lambda\hat{R}_i$ are the LMPs derived from the solution of the master problem. For the rest of the distribution network i, the KKTs are as follows:

$$\begin{aligned}(ne_n) : \lambda_n - \pi e_i + \sum_{k \in K_i} PTDF_{kn}\gamma_k^+ \\ - \sum_{k \in K_i} PTDF_{kn}\gamma_k^- = 0, \quad n \in N_i\end{aligned} \tag{41}$$

$$(nr_n) : \lambda R_n - \pi r_i - \kappa_n = 0, \quad n \in N_i \tag{42}$$

$$0 \le \hat{p}_g \perp MC_g - \lambda_{B_g} + \beta_g \ge 0, \quad g \in US_i \tag{43}$$

$$0 \le \hat{r}_g \perp -\lambda R_{B_g} + \beta_g \ge 0, \quad g \in US_i \tag{44}$$

$$\begin{aligned}0 \le \gamma_k^- \perp - \sum_{n \in N_i} PTDF_{n,k}\hat{ne}_n + \sum_{k' \in K} \max(-A_{k,k'}, 0)\,\hat{fr}_{k'}^+ \\ + \sum_{k' \in K_i} \max(A_{k,k'}, 0)\,\hat{fr}_{k'}^- \le F_k^-, k \in K_i\end{aligned} \tag{45}$$

$$\begin{aligned}0 \le \gamma_k^+ \perp \sum_{n \in N_i} PTDF_{n,k}\hat{ne}_n + \sum_{k' \in K_i} \max(A_{k,k'}, 0)\,\hat{fr}_{k'}^+ \\ + \sum_{k' \in K_i} \max(-A_{k,k'}, 0)\,\hat{fr}_{k'}^- \le F_k^+,\ k \in K_i\end{aligned} \tag{46}$$

$$0 \le \beta_g \perp P_g^{\max} - \hat{p}_g - \hat{r}_g \ge 0, \quad g \in US_i \tag{47}$$

$$\begin{aligned}0 \le \hat{fr}_k^+ \perp \sum_{k' \in K_i} max(A_{k,k'}, 0)\gamma_{k'}^+ \\ + \sum_{n \in N_i : n = FB_k} \kappa_n - \sum_{n \in N_i : n = TB_k} \kappa_n \ge 0,\ k \in K_i\end{aligned} \tag{48}$$

$$\begin{aligned}0 \le \hat{fr}_k^- \perp \sum_{k' \in K_i} \max(A_{k,k'}, 0)\,\gamma_{k'}^- \\ - \sum_{n \in N_i : n = FB_k} \kappa_n + \sum_{n \in N_i : n = TB_k} \kappa_n \ge 0,\ k \in K_i\end{aligned} \tag{49}$$

Proposition 2. *The decentralized pricing method provides identical LMPs with the monolithic problem.*

Proof. The analytical proof is provided in [31]. □

IV. Illustrative Example

A. Alternative Designs

We consider two stylized benchmark designs—*Conservative* and *Aggressive*—that have been examined in our prior collaborations with industry partners [17]. We provide a brief overview of the alternative designs in the remainder of this subsection. The complete formulation is provided in [31].

Conservative design. The conservative design disables all distribution-side flexibility by blocking DSO bids. Formally,

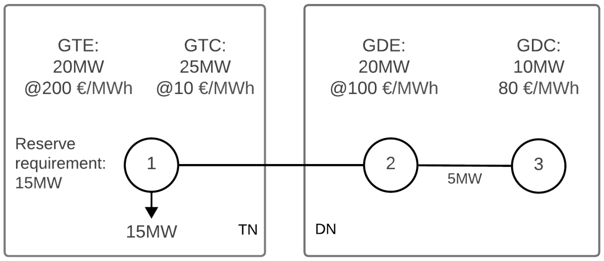

Fig. 5. Illustrative T&D example of Section IV-B. Note that free bids are allowed.

the hierarchical structure is identical to the model presented in Section III-A, with the only exception that the slave subproblems have all the committed reserves r fixed to zero to enforce that no DSO-level resources are activated.

Aggressive design. The aggressive design permits full activation of DSO bids while deliberately neglecting distribution line capacity limits. In relation to the baseline DN formulation in III-A, the line-capacity constraints Eqs. (6), (7) are omitted. This implies that distribution flows are unconstrained and all eligible DSO bids can in principle be cleared in the market.

B. Illustrative Example of T&D Coordination Based on Reserve Deliverability

The behavior of the alternative designs is highlighted in this section with the illustrative example of Fig. 5. In this example, at the transmission level, there is an expensive unit GTE that bids 20MW at a price of 200 €/MWh and a cheap one GTC that bids 25MW at 10 €/MWh, but cannot offer reserve. Similarly, at the distribution level there are two units: an expensive one GDE that bids 20MW at 100 €/MWh and a cheaper one GDC that bids 10MW at 80 €/MWh. A real power flow limit of 5MW is considered on the line that connects GDE with GDC. In the day-ahead timeframe, there is a load of 15MW at the transmission bus and a reserve requirement from the system operator of 15MW. The day-ahead market clears 15MW of reserve from GTE and 15MW of energy from GTC for all the designs. For the balancing market, an imbalance of -9 MW at the transmission bus is assumed and the market clearing results are presented in Table I.

TABLE I
BALANCING MARKET RESULTS BY GENERATOR FOR EACH DESIGN

Market Design	GTE [MW]	GTC [MW]	GDE [MW]	GDC [MW]	Cost [€]
Proposed	0	0	4	5	800
Conservative	9	0	0	0	1800
Aggressive	0	0	0	9	720

For the conservative approach, bids at the distribution level are blocked, leaving only GTE to cover the imbalance in real time. This results in a highly inefficient clearing of the market. On the other extreme, the aggressive design allows the least costly clearing, as GDC covers the entire imbalance, but it comes at the price of overloading the line between GDE and GDC. The proposed design strikes a balance between these two, achieving optimal system security and economic efficiency. GDC is cleared to a level that prevents line overloading, with any remaining imbalance covered by a cheaper distribution resource, GDE, rather than GTE. This outcome aligns exactly with the principles of a well-functioning system: economic efficiency is desirable, but system security is paramount.

V. CASE STUDY

This section details a case study examining transmission-distribution coordination in Belgium. The methodology used to establish this case study is described first, followed by a comparison of the scalability of the decomposed and monolithic models. Subsequently, a comparative analysis is performed between our model and the alternative designs described in section IV-A with respect to a range of metrics of technical and economic relevance. The case study considers both upward and downward reserves. Extending the model of Section II-B to accommodate downward reserves is straightforward: one introduces downward reserve trade variables fr^{dn} and applies the inscribed boxes methodology identically to the case of upward reserves. The complete formulation, along with the corresponding extensions to the LOC and pricing models to accommodate downward reserves, is provided in [31]. We emphasize that our framework uses co-optimization and nodal pricing and applies this design to a Belgian case study. Arguably, US markets are closer to such a design setup. We choose to analyze the Belgian system for reasons of data availability, and we do not expect the choice of precise system to affect the main conclusions of our work regarding scalability, security, incentive alignment and policy insights.

The market models are implemented in Julia v.1.12.4 using JuMP v1.30.0, on the ARIS HPC infrastructure of GRNET. The employed solver is Gurobi 13 for linear programs and Ipopt v1.14.1 for non-convex programs.

A. Setup of case study

Transmission network. The system we study is a realistic representation of the Belgian transmission network, based on a commercial dataset provided by the ENTSO-e TYNDP. The network consists of 628 buses and 725 edges, including lines and transformers. The voltage levels of the examined networks range from 380kV to 12kV. The dataset includes a day-ahead snapshot of load values modeled as price-inelastic power withdrawals. We do not analyze a full 24-hour time series, but rather independent (hourly) time steps that are representative of various sytem conditions. In the absence of intertemporal constraints, every hour of a 24-hour day-ahead planning could be considered independently. Extending the analysis to the case of intertemporal constraints is a direction that will be pursued in future work, see the discussion in section VI.

Transmission level power units. There are 615 generators in the system. It is assumed that all generators provided in the dataset are committed for the given snapshot. Furthermore, the marginal costs are derived from the dataset used in [33]. Moreover, additional generators are incorporated in order to simulate a costly demand response technology that is specifically available for periods of scarcity.

Imports. The commercial dataset also includes the imports of Belgium for the specific snapshot that we are examining. Concretely, imports are modeled as price-inelastic power injections.

ORDC. According to Elia [34], by 2028 the FRR dimensioning for downward reserves is expected to be approximately 1.2 GW, while the anticipated upward reserve requirement for Belgium is expected to reach roughly 2 GW. We derive the ORDCs using the methodology outlined in [35], assuming a mean of 0 MW and a standard deviation of 400 MW. Setting the standard deviation to one third of the downward reserve requirement results in a loss-of-load probability of 0.27% for downward imbalances, which is a level we consider an acceptable reliability standard. The upward ORDC includes a minimum contingency capacity of 800 MW, while mirroring the downward curve beyond that threshold.

Distribution networks. In our analysis, we attach detailed distribution networks to selected transmission nodes. Distribution system load is modeled as a price-inelastic fixed injection, scaled to half the initial load of the corresponding transmission bus. Line resistance, reactance, and capacity limits of each distribution network are similarly scaled according to the initial load of its parent transmission bus. Flexible resources that are derived from Picloflex [36] are assumed to participate in the day-ahead and real-time markets at the distribution level[2]. Using this methodology, 360 DNs are generated from an initial set of 7 unique DNs from [37]. The final T&D network comprises of 112355 buses, 112452 lines and 38443 units.

B. Scalability

In this section, a comparative scalability analysis between the monolithic and the proposed decomposed algorithm across increasing numbers of distribution systems is presented. Using the methodology described previously in section III-A, the size of the dataset is expanded by incorporating additional distribution networks into the transmission system. Leveraging the inherent independence of the Benders subproblems, we parallelize the optimization process across 50 cores on a high performance computing cluster. The results, which are summarized in Table II, demonstrate the advantage of the decomposed algorithm over the monolithic approach in terms of scaling up to systems of arbitrary size. As the system size scales from 50 to 360 distribution networks, the distributed algorithm consistently demonstrates superior scalability in both memory and computational time. Notably, the monolithic method fails due to memory at 150 distribution networks, whereas the distributed algorithm successfully completes the computation even for the instance with 360 distribution networks. This outcome emphasizes the practical limitations of the monolithic approach for large-scale problems and highlights the ability of the distributed algorithm to handle arbitrarily large system instances.

[2]Overall, the bids at the distribution level are more expensive than the transmission system bids, with the exception of the peak technology that we have introduced at the transmission level.

TABLE II
SCALABILITY OF THE DECOMPOSED ALGORITHM VERSUS THE MONOLITHIC FORMULATION.

# of distribution systems	Memory monolithic [GB]	Run time monolithic [sec]	Memory distributed [GB]	Run time distributed [sec]
50	15.3	728	1.19	111.28
100	20.56	3201	1.4	166.75
150	N/A	N/A	1.51	255.52
360	N/A	N/A	2.08	974.29

This is particularly encouraging, since as we explain in [17] our Benders decomposition, developed in section III-A, can be reasonably approximated by an aggregation of bids which are bid into the wholesale market. These bids, which correspond to the residual supply function of the distribution network, coincide with the optimality cuts of the value function of the Benders follower subproblem.

C. Day-ahead Market Clearing Results

This section provides an overview of the day-ahead market-clearing outcomes for each design. Four primary system loading scenarios are examined: (i) Base Case, which represents typical grid conditions; (ii) Scarcity, which represents a case of overall scarcity; (iii) Distribution Oversupply, which represents a scenario where renewable resources in the distribution networks experience oversupply; and (iv) Scarcity and Distribution Oversupply, which represents a case of overall system scarcity (e.g. low transmission-level renewable output and excessive load), while the distribution network renewable resources are producing high output. Table III provides a comprehensive summary of the day-ahead market clearing results, illustrating the quantitative performance of all designs across the four defined scenarios. Specifically, the metrics include: Energy and Reserve$^{up/dn}$ (total cleared quantities), Flow E and Flow R$^{up/dn}$ (energy and reserve flows across the TN-DN interface—positive for TN→DN energy flow and positive for DN→TN reserve flow), and average locational marginal energy and reserve prices π^E, $\pi^{R,up}$, $\pi^{R,dn}$ at both TN and DN levels.

1) Base case: The Proposed and Aggressive designs leverage distribution-level capacity for upward reserves, while the Conservative design diverts transmission resources from energy to reserve provision to compensate for the absence of distribution flexibility, resulting in scarcity of both upward and downward reserves. Distribution reserve prices collapse to 0 €/MWh under the Conservative design, consistent with distribution resources not being committed for providing reserve. The absence of congestion yields uniform energy and reserve prices across the transmission and distribution networks for the remaining designs.

2) DN Oversupply: The surplus of distribution network supply causes an upstream energy flow, with the distribution networks exporting 2.3 GW to the transmission network.

TABLE III
DAY-AHEAD MARKET CLEARING RESULTS.

	Base Case			DN Oversupply			Scarcity			TNS & DNO		
Metric	**Prop.**	**Cons.**	**Aggr.**	**Prop.**	**Cons.**	**Aggr.**	**Prop.**	**Cons.**	**Aggr.**	**Prop.**	**Cons.**	**Aggr.**
Energy [GW]	10.7	10.7	10.7	3.4	3.4	3.4	14.6	14.6	14.6	14.2	14.2	14.2
Reserve^{up} [GW]	2.0	1.78	2	2.0	1.84	2.0	1.6	1.42	1.6	1.67	1.45	1.97
Reserve^{dn} [GW]	1.11	0.98	1.11	1.0	0.92	1.0	1.2	1.2	1.2	1.2	1.2	1.2
Flow E [GW]	5.0	5.0	5.0	-2.3	-2.3	-2.3	5	4.2	5	-2.3	-2.8	-2.3
Flow R^{up} [GW]	0.84	0.0	1.0	0.48	0.0	0.79	1.0	0.0	1.0	0.75	0.0	1.0
Flow R^{dn} [GW]	0.0	0.0	0.0	0.0	0.0	0.0	0.0	0.0	0.0	0.0	0.0	0.0
π_{TN}^{E} [€/MWh]	90.9	90.9	90.9	39.7	39.7	39.7	446	657	446	320.9	582.3	211.2
$\pi_{TN}^{R,up}$ [€/MWh]	0.0	60.9	0.0	0.0	39.2	0.0	193	502	193	124.5	426.9	14.8
$\pi_{TN}^{R,dn}$ [€/MWh]	20.5	56.1	20.5	51	85	51	0.0	0.0	0.0	0.0	0.0	0.0
π_{DN}^{E} [€/MWh]	90.9	90.9	90.9	39.7	39.7	39.7	446	657	446	315	576.5	211.2
$\pi_{DN}^{R,up}$ [€/MWh]	0.0	0.0	0.0	0.0	0.0	0.0	193	0.0	193	118.8	0.0	14.8
$\pi_{DN}^{R,dn}$ [€/MWh]	20.5	0.0	20.5	51	0.0	51	0.0	0.0	0.0	0.0	0.0	0.0

Consequently, energy prices drop to 39.7 €/MWh across all designs. For the Proposed design, the upstream reserve flow acts additively to the energy flow and thus, not all the available reserve is delivered. In contrast, the Aggressive design attempts to provide 0.79 GW of reserve, which exceeds the actual carrying capacity of the distribution infrastructure. The Conservative design remains isolated, maintaining a zero reserve flow.

3) Scarcity: Reduced renewable generation increases the needs of the system for energy, and all designs exhibit scarcity in both reserve products with correspondingly high prices. The Conservative design produces energy with distribution resources to free transmission resources for upward reserve, reducing distribution network energy imports. The remaining designs use distribution resources directly for upward reserve provision.

4) TN Scarcity (TNS) and DN Oversupply (DNO): This scenario combines an increased energy requirement with a surplus of distribution network generation. By disregarding thermal line limits, the Aggressive design clears higher upward reserve volumes from the distribution level, which lowers reserve prices. Because of the no-arbitrage conditions of co-optimization, this also pulls down the energy price: since the marginal cost of the marginal unit is the same with the Proposed, a lower reserve price implies a lower energy price. As in the scenario of distribution network Oversupply, the Proposed design encounters distribution-level congestion. Here, the distribution networks provide the maximum deliverable reserve capacity—inherently lower than the volumes scheduled by the Aggressive design, since the latter permits reserve allocations that exceed physical distribution line capacities.

D. Performance Evaluation: Security, Efficiency, and Incentive Alignment

In this section, we analyze the performance of the designs across three Key Performance Indicators: Incentive alignment (LOC), efficiency (welfare maximization) and security (redispatch quantity). To evaluate efficiency and security, we simulate 100 system imbalances drawn from $\mathcal{N}(0, 400\text{MW})$. The outcomes are summarized in Table IV, which compares the total LOC, total welfare (Welfare), which is a combination of the DA welfare minus the mean of real time operational cost, and mean redispatch quantity across all scenarios for each design.

LOC. In order to calculate the LOC of a given design, we need to compute the difference between the profit that all market agents can earn by self-dispatching against the prices of that design versus the profit that they earn, given those same prices, by following the optimal dispatch of the Proposed design. This indicates how much the prices of alternative designs deviate from inducing the optimal response of resources through price signals. We refer the reader to [31] for the analytical formulation.

As shown in Table IV, the Conservative design produces a substantial LOC across all operational scenarios. The main driving factor is the misalignment between transmission and distribution reserve prices: in the absence of distribution-level congestion, reserve prices at the distribution network collapse to zero while transmission prices remain high. This leads to significant LOC for the network operator, as no arbitrage opportunity should exist for trading reserves across an uncongested distribution network. When solving its own surplus maximization problem, the reserve buyer consumes less reserve than optimal, because of the higher reserve prices in this design. Consequently, following market instructions results in a loss of profit, since the buyer consumes reserves under the optimal dispatch even when the marginal benefit does not exceed the market-clearing price of the Conservative design. Similarly, when generators are solving their own surplus maximization problems, they provide more reserve (and less energy) than required by the optimal dispatch decision due to the high prices, which ultimately results in LOC. This suggests that reserve prices are artificially high under the Conservative design, because the design inefficiently excludes flexible distribution-level agents from the reserve market.

Conversely, while the Aggressive design manages to match the zero LOC of the Proposed design under typical grid

TABLE IV
KPI Comparison across designs and scenarios

	Base Case			DN Oversupply			Scarcity			TNS & DNO		
Metric	**Prop.**	**Cons.**	**Aggr.**	**Prop.**	**Cons.**	**Aggr.**	**Prop.**	**Cons.**	**Aggr.**	**Prop.**	**Cons.**	**Aggr.**
LOC [k€]	0.0	2,557.4	0.0	0.0	3,602.2	0.0	0.0	20,805.0	0.0	0.0	17,761.2	15.8
Welfare [k€]	52,917.3	52,813.9	52,917.3	58,022.26	57,969.27	58,022.26	46,655.1	43,477.7	46,655.1	47,911.2	45,634.8	48,078.2
Re-disp. [MW]	201	201	201	137	137	137	266.3	231.6	266.3	140	148	145

states, the mechanism produces non-zero LOC in the TNS & DNO scenario. The failure to internalize distribution-level congestion results in an LOC of 15.8 thousand €. The network operator experiences no LOC, since there is no locational differentiation in prices, which precludes network operator profits from trading energy or reserve. On the other hand, both the reserve buyer and the generators forego profit when following market instructions as the market procures less reserve from distribution networks because it cannot be physically delivered.

The LOC of the proposed market clearing approach is zero, indicating that the agents have no incentive to deviate from the platform dispatch decisions given the market clearing prices that the design produces. This zero LOC is anticipated by the theory since the market model is convex.

Efficiency. In the Base Case, the Conservative design incurs the highest system cost due to its inability to access cheaper resources from the distribution level when a significant imbalance arises. The Aggressive and Proposed designs perform similarly, because they successfully utilize these cheaper, flexible distribution-level resources. Furthermore, no congestion is caused by energy and reserve flows, since upward reserve and energy flow in opposite directions, and no downward reserve flows into the distribution level.

For the DN Oversupply scenario, the Conservative design again underperforms. In the absence of distribution system flexibility, some TN resources must provide upward reserve, which causes them to undersupply downward reserve. The Aggressive and Proposed designs, on the other hand, perform identically, as the TN resources are adequate for providing cheaper upward and downward activations, meaning congestion at the distribution level has no impact.

Under the Scarcity scenario, the Aggressive and Proposed designs again coincide. Supplying upward reserve does not cause additional loading to the distribution network, and downward reserve flows do not induce congestion. The Conservative design performs significantly worse because valuable distribution-level reserve is withheld from the transmission network, thus resulting in an oversupply of upward reserve under conditions of scarcity.

In the TNS and DNO scenario, the Conservative design again attains the worst performance, due to shortage in distribution-level reserve. The Aggressive design appears to perform better than the Proposed design, because it utilizes lower-cost distribution resources, since it does not account for network constraints. This, however, comes at the cost of network violations and incentive alignment, as reflected in the non-zero LOC and higher redispatch volume of this design under this same scenario.

Security. The designs perform similarly across all scenarios, with the exception of the TNS & DNO case. In the Base Case, all designs require the same amount of redispatch. Because low-cost TN flexible resources are sufficient to meet real-time energy needs, and thus no DN flexibility is activated in the day-ahead or real-time stages, redispatch is largely driven by the need to cover losses across the 360DNs.

Similarly, in the DN Oversupply scenario, even with energy flowing upstream, cheaper transmission network resources can adequately cover imbalances without triggering distribution network resource activation. However, the redispatch volume differs from the Base Case due to network topology: the path for downstream flow to reach loads differs from the path for upstream flow to reach the transmission network, resulting in different amounts of losses on the distribution network. Delivering the scheduled distribution network energy to the transmission network requires activating additional distribution network resources to offset these losses.

In the Scarcity scenario, the Conservative design yields the lowest redispatch volume. The amount differs from the Base Case because, in this scenario, a significant share of distribution network resources is activated for energy in the day-ahead stage, necessitating additional real-time redispatch to cover losses and fulfill those energy commitments. The remaining designs can activate all available distribution capacity, as discussed in the previous KPI, and thus perform identically. Their mean redispatch volumes exceed that of the Conservative design, as the greater utilization of distribution resources in some imbalance realizations requires more additional activations to compensate for losses.

Finally, the designs diverge in the TNS & DNO scenario. The Conservative design requires the highest average redispatch because it activates approximately 500 MW of distribution resources for energy in the DA stage, necessitating substantial loss-compensation redispatch in real time. The remaining designs surpass this volume only when the imbalance realization draws more than 500 MW from distribution resources. Among the two, the Aggressive design incurs higher average redispatch than the Proposed, as large imbalances force the activation of generators without considering congested distribution lines. The Proposed design performs best overall: it avoids congestion-driven redispatch and requires less redispatch than the Conservative approach whenever the imbalance does not severely stress the system.

VI. Conclusions

This paper proposes a day-ahead and real-time design for TSO–DSO coordination, and compares it on the basis of economic and technical metrics to two alternatives that have been considered by industry. The proposed model includes reserve deliverability constraints, and relies on a decentralized computation and information framework for computing market clearing dispatch and prices. Its effectiveness is demonstrated on a realistic case study of Belgium comprising thousands of buses and distributed energy resources, where we establish scalability relative to a monolithic formulation and confirm incentive alignment through a zero lost opportunity cost metric across all loading scenarios. We further demonstrate that our proposed approach strikes the most favorable balance between efficiency and security relative to the alternatives.

Beyond the current implementation, future research directions include the extension to multi-period optimization to capture temporal dependencies. In such settings, the LOC metric remains a relevant indicator of incentive alignment for multi-period horizons. Non-convexities arising from unit commitment constraints are also a relevant direction of future work. Subsequent efforts will explore less conservative alternatives to the inscribed boxes approach, extending the applicability of the framework to non-radial distribution networks and incorporating alternative power flow representations [38].

ACKNOWLEDGEMENT

This work has received funding from the European Research Council (ERC) under the European Union Horizon 2020 Research and Innovation Programme (grant agreement No.850540). Moreover, it was supported by computational time granted from the National Infrastructures for Research and Technology S.A. (GRNET) in the National HPC facility - ARIS - under project ID pr019005_fat.

REFERENCES

[1] S. Chondrogiannis, J. Vasiljevska, A. Marinopoulos, I. Papaioannou, and G. Flego, "Local electricity flexibility markets in Europe," Tech. Rep., 2022, [Link].

[2] Z. Ruan, A. Papavasiliou, and M. Madani, "Distribution Locational Marginal Pricing under Generation and Network Scarcity Conditions," *Current Sustainable/Renewable Energy Reports*, vol. 12, no. 1, p. 33, 2025. [Online]. Available: https://doi.org/10.1007/s40518-025-00282-9

[3] M. Madani, A. Papavasiliou, and Z. Ruan, "The Inscribed Boxes Approach to Reserve Deliverability in Balancing Capacity Markets: Base Results," in *2025 21st International Conference on the European Energy Market (EEM)*, 2025, pp. 1–6.

[4] Frontier Economics (for ENTSO-e), "Review of Flexibility Platforms," Tech. Rep., 2021, [Link].

[5] T. Schittekatte and L. Meeus, "Flexibility markets: Q&A with project pioneers," *Utilities Policy*, vol. 63, 4 2020.

[6] S. Potenciano Menci and O. Valarezo, "Decoding design characteristics of local flexibility markets for congestion management with a multi-layered taxonomy," *Applied Energy*, vol. 357, pp. 122–203, 2024.

[7] M. Caramanis, E. Ntakou, W. W. Hogan, A. Chakrabortty, and J. Schoene, "Co-Optimization of Power and Reserves in Dynamic T&D Power Markets With Nondispatchable Renewable Generation and Distributed Energy Resources," *Proceedings of the IEEE*, vol. 104, no. 4, pp. 807–836, 2016.

[8] G. T. Heydt, B. H. Chowdhury, M. L. Crow, D. Haughton, B. D. Kiefer, F. Meng, and B. R. Sathyanarayana, "Pricing and Control in the Next Generation Power Distribution System," *IEEE Transactions on Smart Grid*, vol. 3, no. 2, pp. 907–914, 2012.

[9] R. Li, Q. Wu, and S. S. Oren, "Distribution Locational Marginal Pricing for Optimal Electric Vehicle Charging Management," *IEEE Transactions on Power Systems*, vol. 29, no. 1, pp. 203–211, 2014.

[10] A. Papavasiliou, "Analysis of Distribution Locational Marginal Prices," *IEEE Transactions on Smart Grid*, vol. 9, no. 5, pp. 4872–4882, 2018.

[11] S. Huang, Q. Wu, S. S. Oren, R. Li, and Z. Liu, "Distribution Locational Marginal Pricing Through Quadratic Programming for Congestion Management in Distribution Networks," *IEEE Transactions on Power Systems*, vol. 30, no. 4, pp. 2170–2178, 2015.

[12] Z. Yuan, M. R. Hesamzadeh, and D. R. Biggar, "Distribution Locational Marginal Pricing by Convexified ACOPF and Hierarchical Dispatch," *IEEE Transactions on Smart Grid*, vol. 9, no. 4, pp. 3133–3142, 2018.

[13] L. Bai, J. Wang, C. Wang, C. Chen, and F. Li, "Distribution Locational Marginal Pricing (DLMP) for Congestion Management and Voltage Support," *IEEE Transactions on Power Systems*, vol. 33, no. 4, pp. 4061–4073, 2018.

[14] W. W. Hogan, "Electricity Scarcity Pricing Through Operating Reserves," *Economics of Energy and Environmental Policy*, vol. 2, 2013.

[15] K. Neuhoff, F. Klaucke, L. Olmos, L. Ryan, S. Vitiello, A. Papavasiliou, and K. Staschus, "EU power market reform toward locational pricing: Rewarding flexible consumers for resolving transmission constraints," *Energy Policy*, vol. 207, p. 114808, 2025, [Link].

[16] MCSC SDAC, "Co-optimisation of Energy and Balancing Capacity in SDAC Phase 1 R&D Report (R0) on Bidding Products, Bid Design and Pricing," MCSC SDAC, s.l., Tech. Rep., 2025.

[17] N-SIDE, "Market approaches for TSO-DSO coordination in Norway," Tech. Rep., 2021, [Link].Accessed: May 11, 2026.

[18] H. Gerard, E. Rivero, and D. Six, "Basic schemes for TSO-DSO coordination and ancillary services provision," Smartnet, Tech. Rep., 2016.

[19] Z. Yuan and M. R. Hesamzadeh, "Hierarchical coordination of TSO-DSO economic dispatch considering large-scale integration of distributed energy resources," *Applied Energy*, vol. 195, pp. 600–615, 2017.

[20] A. Mohammadi, M. Mehrtash, and A. Kargarian, "Diagonal Quadratic Approximation for Decentralized Collaborative TSO+DSO Optimal Power Flow," *IEEE Transactions on Smart Grid*, vol. 10, no. 3, pp. 2358–2370, 2019.

[21] I. Mezghani, N. Stevens, A. Papavasiliou, and D. I. Chatzigiannis, "Hierarchical Coordination of Transmission and Distribution System Operations in European Balancing Markets," *IEEE Transactions on Power Systems*, vol. 38, no. 5, pp. 3990–4002, 2023.

[22] T. Jiang, C. Wu, R. Zhang, X. Li, H. Chen, and G. Li, "Flexibility Clearing in Joint Energy and Flexibility Markets Considering TSO-DSO Coordination," *IEEE Transactions on Smart Grid*, vol. 14, no. 2, pp. 1376–1387, 2023.

[23] M. A. Bragin and Y. Dvorkin, "TSO-DSO Operational Planning Coordination Through "l_1-Proximal" Surrogate Lagrangian Relaxation," *IEEE Transactions on Power Systems*, vol. 37, no. 2, pp. 1274–1285, 2022.

[24] T. Zheng and E. Litvinov, "Contingency-Based Zonal Reserve Modeling and Pricing in a Co-Optimized Energy and Reserve Market," *IEEE Transactions on Power Systems*, vol. 23, no. 2, pp. 277–286, 2008.

[25] Z. Zhao, Y. Liu, L. Guo, L. Bai, Z. Wang, and C. Wang, "Distribution Locational Marginal Pricing Under Uncertainty Considering Coordination of Distribution and Wholesale Markets," *IEEE Transactions on Smart Grid*, vol. 14, no. 2, pp. 1590–1606, 2023.

[26] J. D. Lyon, K. W. Hedman, and M. Zhang, "Reserve Requirements to Efficiently Manage Intra-Zonal Congestion," *IEEE Transactions on Power Systems*, vol. 29, no. 1, pp. 251–258, 2014.

[27] N. G. Cobos, J. M. Arroyo, and A. Street, "Least-Cost Reserve Offer Deliverability in Day-Ahead Generation Scheduling Under Wind Uncertainty and Generation and Network Outages," *IEEE Transactions on Smart Grid*, vol. 9, no. 4, pp. 3430–3442, 2018.

[28] A. Paredes, J. A. Aguado, and P. Rodríguez, "Uncertainty-Aware Trading of Congestion and Imbalance Mitigation Services for Multi-DSO Local Flexibility Markets," *IEEE Transactions on Sustainable Energy*, vol. 14, no. 4, pp. 2133–2146, 2023.

[29] S. S. Oren, *Point to Point and Flow-Based Financial Transmission Rights: Revenue Adequacy and Performance Incentives*. London: Springer London, 2013, pp. 77–94. [Online]. Available: https://doi.org/10.1007/978-1-4471-4787-9_3

[30] M. Garcia, H. Nagarajan, and R. Baldick, "Generalized Convex Hull Pricing for the AC Optimal Power Flow Problem," *IEEE Transactions on Control of Network Systems*, vol. 7, no. 3, pp. 1500–1510, 2020.

[31] Z. Ruan, A. Papavasiliou, and D. Krithis, "Appendix of A TSO-DSO Coordination Platform on AC Networks with Reserve Deliverability," [Link].Accessed: May 10,2026.

[32] Benders, J. F., "Partitioning procedures for solving mixed-variables programming problems," *Numerische Mathematik*, vol. 4, pp. 238 – 252, 1962.

[33] I. Aravena and A. Papavasiliou, “Renewable Energy Integration in Zonal Markets,” *IEEE Transactions on Power Systems*, vol. 32, no. 2, pp. 1334–1349, 2017.
[34] ELIA Group, “MOGII System integration study,” 2020, [Link].Accessed: May 5, 2026.
[35] A. Papavasiliou, *Optimization Models in Electricity Markets*. Cambridge University Press, 2024.
[36] Piclo, “About,” 2025, [Link].Accessed: Nov. 5, 2025.
[37] SEDG, “United Kingdom Generic Distribution System (UKGDS),” [Link], Accessed: May 10,2026.
[38] N. Li, L. Chen, and S. H. Low, “Exact convex relaxation of OPF for radial networks using branch flow model,” in *2012 IEEE Third International Conference on Smart Grid Communications (SmartGridComm)*, 2012, pp. 7–12.

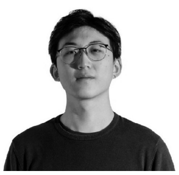

Zejun Ruan received his joint B.Sc./M.Sc. degree in Electrical and Computer Engineering from the National Technical University of Athens (NTUA), Athens, Greece, in 2023. He is currently pursuing the Ph.D. degree with the Energy Systems Laboratory, NTUA, under the supervision of Prof. Anthony Papavasiliou. His research interests include congestion management, optimal power flow, TSO–DSO coordination, and the integration of renewable energy into power systems.

Anthony Papavasiliou (Senior Member, IEEE) is an associate professor at the department of Electrical and Computer Engineering at the National Technical University of Athens. Formerly, he was an associate professor at the Center for Operations Research and Econometrics (CORE) at the Université catholique de Louvain, where he held the ENGIE Chair and a Francqui Research Professorship. He completed his PhD and post-doctoral research at the department of Industrial Engineering and Operations Research at UC Berkeley and his undergraduate studies at the National Technical University of Athens, Greece. In 2026 Anthony received the Dieter Schwartz Courageous Research Grant of the Institute of Advanced Studies at the Technical University of Munich. In 2021 he received the Bodossaki Foundation Distinguished Young Scientist award in Applied Sciences. He is a recipient of an ERC Starting Grant in 2019. He is serving as an associate editor for Operations Research and has served as an Associate Editor for the IEEE Transactions on Power Systems, as well as in the technical program committees of various international conferences. He has received the 2015 INFORMS best publication award in energy. He has served as a consultant for transmission system operators, regulatory authorities, power exchanges, and utilities on a number of topics related to electricity markets and power system operations.

Dimitris Krithis is a PhD candidate at the Division of Electric Power at the National Technical University of Athens (NTUA). He completed his undergraduate studies at NTUA in 2025, obtaining a diploma in Electrical and Computer Engineering. He has work experience in power systems modeling and renewable energy integration. His research interests include electricity markets design and analysis, power system modeling and optimal power flow.